phrp
OSONG PUBLIC HEALTH AND RESEARCH PERSPECTIVES

pISSN 2210-9099 eISSN 2233-6052
https://doi.org/10.24171/j.phrp.2024.0026
Osong Public Health Res Perspect 2024;15(4):286-306

Original Article

Novel prophylactic and therapeutic multi-epitope vaccine based on Ag85A, Ag85B, ESAT-6, and CFP-10 of *Mycobacterium tuberculosis* using an immunoinformatics approach

Muhammad Fikri Nugraha[1], Daniel Alexander Changestu[1], Rizky Ramadhan[1], Tasya Salsabila[1], Arsila Nurizati[1], Sari Eka Pratiwi[2], Ysrafil Ysrafil[3]

[1]Medical Program, Faculty of Medicine, Universitas Tanjungpura, Pontianak, Indonesia
[2]Department of Biology and Pathobiology, Faculty of Medicine, Universitas Tanjungpura, Pontianak, Indonesia
[3]Department of Pharmacotherapy, Faculty of Medicine, Universitas Palangka Raya, Palangka Raya, Indonesia

ABSTRACT

Objectives: Current tuberculosis (TB) control strategies face limitations, such as low antibiotic treatment compliance and a rise in multidrug resistance. Furthermore, the lack of a safe and effective vaccine compounds these challenges. The limited efficacy of existing vaccines against TB underscores the urgency for innovative strategies, such as immunoinformatics. Consequently, this study aimed to design a targeted multi-epitope vaccine against TB infection utilizing an immunoinformatics approach.

Methods: The multi-epitope vaccine targeted Ag85A, Ag85B, ESAT-6, and CFP-10 proteins. The design adopted various immunoinformatics tools for cytotoxic T lymphocyte (CTL), helper T lymphocyte (HTL), and linear B lymphocyte (LBL) epitope prediction, the assessment of vaccine characteristics, structure modeling, population coverage analysis, disulfide engineering, solubility prediction, molecular docking/dynamics with toll-like receptors (TLRs), codon optimization/cloning, and immune simulation.

Results: The multi-epitope vaccine, which was assembled using 12 CTL, 25 HTL, and 21 LBL epitopes associated with CpG adjuvants, showed promising characteristics. The immunoinformatics analysis confirmed the antigenicity, immunogenicity, and lack of allergenicity. Physicochemical evaluations indicated that the proteins were stable, thermostable, hydrophilic, and highly soluble. Docking simulations suggested high-affinity binding to TLRs, including TLR2, TLR4, and TLR9. *In silico* immune simulation predicted strong T cell (cytokine release) and B cell (immunoglobulin release) responses.

Conclusion: This immunoinformatics-designed multi-epitope vaccine targeting Ag85A, Ag85B, ESAT-6, and CFP-10 proteins showed promising characteristics in terms of stability, immunogenicity, antigenicity, solubility, and predicted induction of humoral and adaptive immune responses. This suggests its potential as a prophylactic and therapeutic vaccine against TB.

Keywords: Multi-epitope vaccine; Prophylaxis tuberculosis vaccine; Therapeutic tuberculosis vaccine

Received: January 19, 2024
Revised: April 22, 2024
Accepted: May 26, 2024

Corresponding author:
Sari Eka Pratiwi
Department of Biology and Pathobiology, Faculty of Medicine, Universitas Tanjungpura, Prof. H. Hadari Nawawi street, Pontianak, West Kalimantan, Indonesia, 78124
E-mail: sariekapratiwi@medical.untan. ac.id

Introduction

Tuberculosis (TB) affects 10.6 million people and results in 1.3 million deaths worldwide. Indonesia has the second-highest number of TB cases globally, with an estimated 809,000 patients [1]. The lengthy treatment duration and drug side effects often deter patient adherence [2]. The emergence of multidrug-resistant TB and extensively drug-resistant TB further complicates treatment, necessitating increased funding [3]. These challenges significantly hinder the achievement of the goal of eliminating TB cases by 2030, as outlined in Sustainable Development Goal 3 [4,5].

Preventive and curative efforts are paramount in addressing the rising number of TB cases and deaths. However, the Bacillus Calmette-Guérin vaccine for children is solely preventive and demonstrates limited effectiveness in adults and those already infected [3]. Several new vaccines, such as MTBVAC, GamTBvac, and M72/AS01E—which combines the M72 protein fusion with the AS01E adjuvant—are currently undergoing clinical trials. However, these vaccines' ability to induce and activate CD4+ T lymphocytes, CD8+ T lymphocytes, and B lymphocytes remains to be confirmed. Consequently, there is an urgent need for vaccines that can effectively stimulate these immune cells, potentially through innovative approaches like immunoinformatics [6].

Developing prophylactic and therapeutic vaccines using immunoinformatics represents a novel strategy. The identification of immunogenic T cell and B cell peptides/epitopes from *Mycobacterium tuberculosis* proteins can accelerate the discovery of multi-epitope vaccine candidates [7,8]. Several *M. tuberculosis* proteins, including Ag85, ESAT-6, and CFP-10, are potential vaccine candidates. The Ag85 protein, consisting of Ag85A, B, and C, plays a significant role in bacterial defense against the immune system by forming tubercles [9]. Meanwhile, the ESAT-6 protein inhibits autophagy and induces macrophage apoptosis by activating caspase expression and lysing phagosomal membranes. Damage to ESAT-6 is linked with the repair of auto-phagolysosomal fusion in DCs in response to *M. tuberculosis*. Similarly, the CFP-10 protein reduces the production of nitric oxide and reactive oxygen species and inhibits macrophages' ability to kill [10].

Recent studies on protein-based vaccines have shown promising results, particularly with Ag85B and ESAT-6. Vaccines targeting these proteins have successfully completed phase I trials, demonstrating both immunogenic and therapeutic efficacy in adults who are sensitive or resistant to multiple antibiotics [11]. Additionally, a vaccine that combines Ag85A, ESAT-6, and CFP-10 has been shown to improve both humoral and cellular immune responses. This vaccine has progressed to phase II trials and is scheduled for phase III trials [12].

HIGHLIGHTS

- Addressing the tuberculosis (TB) burden: This study focuses on the significant TB burden in Indonesia, which is the second-largest contributor to TB-related deaths worldwide. Given the limited efficacy of the current Bacillus Calmette-Guérin vaccine, we investigated a novel multi-epitope vaccine that utilizes promising protein antigens from *Mycobacterium tuberculosis*.
- Novelty of the vaccine: The novel vaccine combines epitopes from Ag85A, Ag85B, ESAT-6, and CFP-10, potentially triggering potent humoral and cellular immune responses.
- Potential results: The vaccine exhibits desirable properties including immunogenicity, non-allergenicity, antigenicity, and robust interaction with key immune receptors (toll-like receptor [TLR] 2, TLR4, TLR9). The multi-epitope strategy aids in both the prevention of TB infections (prophylactic) and the treatment of existing cases (therapeutic).

This study aimed to develop a multi-epitope vaccine targeting *M. tuberculosis* proteins Ag85A, Ag85B, ESAT-6, and CFP-10 through immunoinformatics analysis. The vaccine candidate was designed to meet established standards, being antigenic, immunogenic, non-allergenic, non-toxic, and having favorable physicochemical properties. Additionally, it is expected to stimulate the production of immunoglobulin, IFN-γ, IL-4, and IL-10, offering both prophylactic and therapeutic benefits against TB.

Materials and Methods

Selection of Protein Antigens and Sequence Retrieval

Based on prior studies, Ag85A (P9WQP3.1), Ag85B (A5U3Q3.1), ESAT-6 (AHN50413.1), and CFP-10 (P9WNK5.1) were identified as promising candidates for a multi-epitope vaccine against *M. tuberculosis* [7]. The sequences were retrieved from the National Center for Biotechnology Information (NCBI) database (https://www.ncbi.nlm.nih.gov/). To assess the potential antigenicity of the proteins, the sequences were analyzed using Vaxijen 2.0 web tools (http://www.ddg-pharmfac.net/vaxijen/VaxiJen/VaxiJen.html), adopting a bacterial antigenicity threshold of 0.5. Subsequently, the physicochemical properties of the proteins were evaluated using ProtParam web tools

(https://web.expasy.org/ protparam/).

T Lymphocyte Epitope Prediction

T-cell epitope prediction, which includes both cytotoxic and helper T cells, plays a crucial role in vaccine design by facilitating the activation of adaptive immune system cells. This process involves the presentation of antigenic peptides to T cell receptors via major histocompatibility complex (MHC) molecules [13]. This prediction focused on cytotoxic T lymphocytes (CTLs) (http://tools.iedb.org/mhci/) and helper T lymphocytes (HTLs) (http://tools.iedb.org/mhcii/). CTL epitopes, identified using IEDB NetMHCpan 4.0 with percentiles lower than 2 and 9-mer length constraints, were further evaluated for immunogenicity, antigenicity, allergenicity, and toxicity through dedicated web tools (IEDB Class I Immunogenicity [http://tools.iedb.org/immunogenicity/], VaxiJen 2.0, AllergenFP 1.0 [https://www.ddg-pharmfac.net/AllergenFP/], AllerTOP 2.0 [https://ddg-pharmfac.net/AllerTOP/], and Toxinpred [https://webs.iiitd.edu.in/raghava/toxinpred/design.php]). HTL epitopes were predicted by IEDB NetMHCIIpan 4.1 with percentiles lower than 2 and 15-mer length, followed by similar assessments for antigenicity, allergenicity, and toxicity (VaxiJen 2.0, AllergenFP 1.0, AllerTOP 2.0, Toxinpred). Additionally, specific cytokine secretion potential (IFN-γ, IL-4, IL-10) was predicted for HTL epitopes using the IFNepitop, IL4pred, and IL10pred web tools.

Linear B Cell Epitope Prediction

In the immune system, certain antigen fragments known as B cell epitopes act as receptors that identify infected cells and initiate various immune responses, including the activation of humoral immunity through the production of specific antibodies [14]. Linear B lymphocyte (LBL) epitopes were predicted using ABCpred web tools. The epitopes underwent antigenicity, allergenicity, toxicity, and immunoglobulin analysis using VaxiJen v.2.0, AllergenFP v.1.0, AllerTOP v.2.0, Toxinpred, and Igpred web tools, respectively.

Population Coverage Analysis of T-Cell Epitopes

Population coverage analysis is crucial in the design and development of epitope-based vaccines due to the significant polymorphism of HLA molecules in the peptide-binding region [13]. The population coverage of T-cell epitopes was predicted using the IEDB population coverage (http://tools.iedb.org/population/). This analysis involved specifying the number of epitopes, enabling the calculation option for both MHC class I and II combinations, and selecting the specific area or population for which T-cell epitope coverage was predicted.

Multi-Epitope Vaccine Construction and Evaluation

Multi-epitope vaccine constructs were assembled by linking CTL, HTL, and LBL epitopes using linkers EAAAK (Glu-Ala-Ala-Ala-Lys), GPGPG (Gly-Pro-Gly-Pro-Gly), AAY (Ala-Ala-Tyr), and KK (Lys-Lys). His-tags (HHHHHH) were added at the C-terminal of the protein. Additionally, the CpG ODN protein was incorporated as an adjuvant to enhance immune activation, connected via the EAAAK linker at the beginning of the construct. The vaccine constructs were evaluated for antigenicity, allergenicity, and physicochemical properties using the Vaxijen 2.0, AllergenFP v.1.0, AllerTOP v.2.0, and Protparam web tools.

Prediction of the Secondary and Tertiary Structure of the Multi-Epitope Vaccine

The secondary or 2-dimensional (2D) structure of the vaccine was predicted using PSIPRED web tools (http://bioinf.cs.ucl.ac.uk/psipred/). Furthermore, the tertiary or 3-dimensional (3D) structure was predicted through the I-TASSER server (https://zhanggroup.org/I-TASSER/about.html) and visualized utilizing PyMOL (http://www.pymol.org/pymol).

Multi-Epitope Vaccine 3D Structure Refinement and Validation

The selected 3D structures obtained from the I-TASSER server were refined using the GalaxyRefine server (http://galaxy.seoklab.org/cgi-bin/submit.cgi?type=REFINE). Furthermore, Z-score evaluation was conducted using the ProSA server (https://prosa.services.came.sbg.ac.at/prosa.php). Structural analysis validation and verification (SAVE) (https://saves.mbi.ucla.edu/) was performed for ERRAT value analysis and Ramachandran plots (saves.mbi.ucla.edu).

Prediction of Vaccine Solubility

The vaccine's solubility was determined using online web tools, including a Protein-sol server (https://protein-sol.manchester.ac.uk/). It was further compared with *Escherichia coli* proteins, which have an estimated solubility of 0.45. A score exceeding 0.45 indicated protein solubility. Solubility confirmation was conducted using SOLpro (http:// scratch.proteomics.ics.uci.edu/) with a cut-off score ≥ 0.5.

Disulfide Characterization of the Vaccine Construct

To improve the stability of the protein structure, we analyzed disulfide bridge formation to increase the free energy of the denatured state while reducing conformational entropy. We utilized the online tool Disulfide by Design 2.0 (DbD2) (http://cptweb.cpt.wayne.edu/DbD2/) to facilitate the design of disulfide bonds in the vaccine construct by substituting

https://doi.org/10.24171/j.phrp.2024.0026

particular amino acids with cysteine in high-mobility and unstable regions of proteins. Default settings were applied, including intra-chain, inter-chain bonding, and building Cβ for Gly. Additionally, chi^3 values were set within the range of −87° to +97° (set 30), while Cα–Cβ–Sγ angles (114.6°) were fixed at 10 to ensure accurate bond prediction. The energy value obtained was ensured to be <2.2 for optimal stability [13,15].

Analysis of Discontinuous B Cell Epitopes

Discontinuous B cell epitopes were identified using ElliPro in IEDB (http://tools.iedb.org/ellipro/) based on the 3D protein structure. Default settings, including a minimum score of 0.5 and a maximum distance of 6 Å were used [15].

Analysis of Active Sites in the Vaccine Construct

Active sites in the vaccine structure were analyzed before molecular docking. Initially, polar hydrogens were added to the refined vaccine using Biovia Discovery Studio. Subsequently, the ligand-binding region of the vaccine was analyzed using the Computed Atlas of Surface Topography of Proteins (CASTp 3.0) webserver (http://sts.bioe.uic.edu/castp/index.html? 3igg) with default settings [15].

Molecular Docking of the Multi-Epitope Vaccine

Molecular docking analysis is crucial for assessing the interactions between a vaccine construct and a target protein. In this study, we focused on 3 key proteins in the immune response to *M. tuberculosis*: toll-like receptor (TLR) 2 (2Z7X), TLR4 (4G8A), and TLR9 (5ZLN). The PDB files (https://www.rcsb.org) for these proteins were retrieved from the Protein Data Bank (PDB). Before docking, the vaccine and TLRs were prepared by removing all non-protein molecules, such as water and ligands. Additionally, one chain from each protein was selected for docking with the vaccine: chain A for TLR2 and TLR4, and chain B for TLR9, identified as the optimal attachment sites for the ligand. This preparation also included the addition of polar hydrogens. Docking of the TLRs with the vaccine was performed using several web-based tools, including ClusPro 2.0 (https://cluspro.bu.edu/), which ranks protein complex clusters based on the lowest energy level scores. The best complex models were further refined using HADDOCK 2.4 (https://wenmr.science.uu.nl/haddock2.4/). Finally, the docked protein was assessed for binding free energy (ΔG) using PRODIGY (https://wenmr.science.uu.nl/prodigy/). The docking results were further visualized by the PDBsum server (https://www.ebi.ac.uk/thornton-srv/databases/pdbsum/) and PyMOL. Protein interactions were also analyzed using HDock (http://hdock.phys.hust.edu.cn/) as a semi-flexible approach to predict the binding mode and affinity [16–20].

Molecular Dynamics and MM-GBSA Calculation

The best molecular docking models of TLR with the vaccine construct were further analyzed for molecular dynamics using the iMODs web server (https://imods.iqf.csic.es/). This tool uses normal modes analysis (NMA) in internal coordinates to determine the stability of interaction. Meanwhile, the binding free energy of TLR with the vaccine was estimated using the MM-GBSA approach in HawkDock (http://cadd.zju.edu.cn/hawkdock/). The analysis also adopted the best docking models, and the tools were set to default parameters. The flexibility of protein complexes was analyzed using CABS-flex (https://biocomp.chem.uw.edu.pl/CABSflex2/) [19–22].

Codon Optimization and *In Silico* Cloning of the Multi-Epitope Vaccine

Codon optimization, which involved analyzing the codon adaptation index (CAI) and GC value of the improved sequences, was performed using JCat (https://www.jcat.de/) or IDT (Integrated DNA Technologies) server (https://sg.idtdna.com/pages/tools/codon-optimization-tool). Subsequently, *in silico* cloning was performed on Pet28(A) vectors using Snapgene v4.2 (https://www.snapgene.com/).

Immune Simulation

Immune simulation after multi-epitope vaccine injections was conducted using the C-IMMSIM server (https://kraken.iac.rm.cnr.it/C-IMMSIM/). Three vaccine injections were simulated at 4-week intervals (1, 28, and 56 days).

Results

Retrieval of *Mycobacterium tuberculosis* Protein Sequences

CTL epitope prediction was conducted using the IEDB NetMHCpan EL 4.1 server, setting the percentile thresholds at ≤2 and the epitope length at 9 sequences. Nine widely distributed HLA alleles were selected, including A*0101, A*0201, A*0206, A*0301, A*1101, A*2402, A*2601, A*3101, and A*3303 [23]. Additionally, the epitope prediction included several other alleles deemed significant for TB vaccine development, such as HLA-A*01:01, HLA-A*24:02, HLA-A*26:01, HLA-A*31:01, HLA-A*68:02, HLA-B*07:02, HLA-B*14:02, HLA-B*18:01, HLA-B*27:02, HLA-B*27:05, HLA-A*29:02, HLA-B*49:01, HLA-C*04:01, and HLA-C*07:02 [24]. Furthermore, CTL epitopes with a percentile of ≤2 were further evaluated for immunogenicity, antigenicity, allergenicity, and toxicity. Vaccine candidates were

identified based on their immunogenicity, an antigenicity threshold of ≥0.5, absence of allergenicity as determined by both AllergenFP and AllerTOP 2.0 platforms, and non-toxicity. Detailed results of the CTL epitope prediction analysis are provided in Table S1 as supporting information. In total, 12 epitopes from 4 proteins were found suitable for multi-epitope vaccine construction.

Helper T-Cell Epitope Prediction

HTL epitopes from the *M. tuberculosis* proteins Ag85A, Ag85B, ESAT-6, and CFP-10 were selected using the IEDB MHC-II platform. The criteria set included a percentile of ≤2, an epitope length of 15 sequences, and 27 HLA MHC class II alleles [23,25,26]. Furthermore, HTL epitopes meeting the ≤2 percentile criterion were evaluated for antigenicity, allergenicity, toxicity, and their ability to induce IL-4, IL-10, and IFN-γ. Vaccine candidates were chosen based on several factors: an antigenicity threshold of ≥0.5, no allergenicity as determined by both the AllergenFP and AllerTOP 2.0 platforms, non-toxicity, and the capability to induce IL-4, IL-10, and IFN-γ. In total, 25 HTL epitopes from the proteins Ag85A, Ag85B, ESAT-6, and CFP-10 were identified. The breakdown of selected HTL epitopes includes 14 for Ag85A, 7 for Ag85B, and 4 for CFP-10 (Table S2).

Linear B Cell Epitope Prediction

LBL epitopes for the *M. tuberculosis* proteins Ag85A, Ag85B, ESAT-6, and CFP-10 were predicted using the ABCpred server, with a threshold value set at ≥0.5 and epitope lengths of 16 amino acid sequences. Furthermore, the selected LBL epitopes were identified for antigenicity, allergenicity, toxicity, and immunoglobulin values. Vaccine candidates were selected based on antigenicity (≥0.5 threshold), absence of allergenicity on both AllergenFP and AllerTOP 2.0 platforms, non-toxicity, and the ability to induce immunoglobulins (IgG, IgA, IgE) [27]. The identified LBL epitopes comprised 7 from Ag85A, 9 from Ag85B, an epitope for ESAT-6, and 4 from CFP-10 (Table S3).

Multi-Epitope Vaccine Construction from the Selected Epitopes

Multi-epitope vaccine constructs were developed using selected CTL, HTL, and LBL epitopes, incorporating adjuvants, linkers, and his-tags. The adjuvant, CpG protein ODN, was attached to the N-terminal of the vaccine construct via an EAAAK linker. Additionally, various linkers such as GPGPG for the HTL epitope, KK for the LBL epitope, and AAY for the CTL epitope were integrated into the construct for the proper presentation and separation of epitopes (Figure 1).

Evaluation of the Vaccine's Allergenicity, Antigenicity, and Physicochemical Characteristics

Using the ProtParam website, the multi-epitope vaccine construct, along with the adjuvant, consisted of 1049 amino acids that were antigenic at a score of 1.0642 and non-allergenic. This suggested minimal potential for allergic reactions upon administration [28]. The construct's molecular weight was 102,385 Da, which facilitates an easier purification process, as it falls within the optimal range of 40 to 110 kDa for vaccine development. It exhibited a theoretical isoelectric point (pI) of 9.57, indicating the basic nature of the construct, and had extinction coefficients of 124.930 and 124.680. The estimated half-life of the construct was 30 hours in mammals *in vitro*, over 20 hours in yeast *in vivo*, and over 10 hours in *E. coli in vivo*. This suggests that the vaccine will be stable *in vivo*, allowing prolonged exposure to the immune system and potentially enhancing immune responses [29]. Furthermore, the instability index was calculated as 31.66, implying post-expression stability of the vaccine construct and favorable immunogenicity and immune polarization [30]. It possessed an aliphatic index of 63.66, signifying thermostability, and a grand average of hydropathicity (GRAVY) score of −0.145, indicative of the vaccine's hydrophilic nature (Table 1).

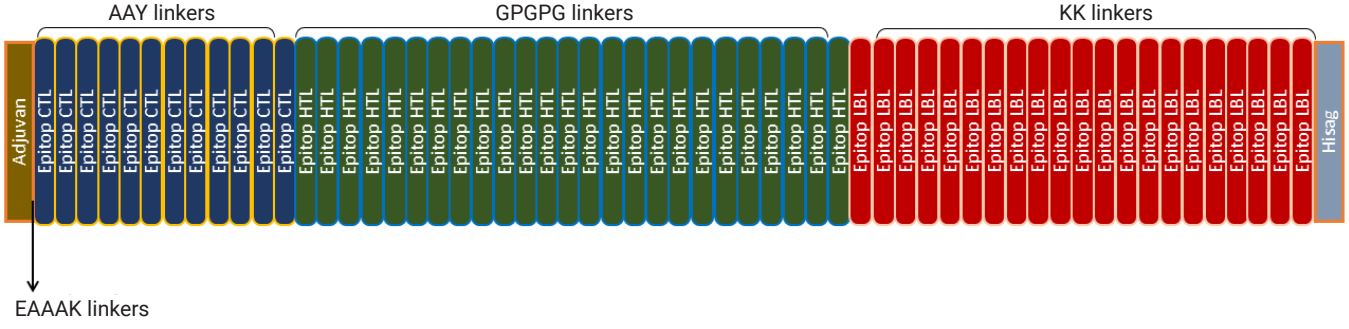

Figure 1. Multi-epitope vaccine construct design template.
EAAAK, Glu-Ala-Ala-Ala-Lys; GPGPG, Gly-Pro-Gly-Pro-Gly; AAY, Ala-Ala-Tyr; KK, Lys-Lys.

https://doi.org/10.24171/j.phrp.2024.0026

Table 1. Antigenicity, allergenicity, and physicochemical characteristic of the vaccine construct

Construction	Antigenicity	Allergenicity	Molecular weight	Theoretical pI	Ext. coefficient	Est. half life	Instability index	Aliphatic index	GRAVY
Adjuvant (1049 AA)	1.0642	Probable non-allergen	102.385 Da	9.57 (basic)	124.930, 124.680	Mammals, *in vitro*: 3 h; yeast, *in vivo*: >20 h; *E. coli*, *in vivo*: >10 h	31.66 (stable)	63.66 (thermostable)	−0.145

pI, isoelectric point; GRAVY, grand average of hydropathicity; AA, amino acid; *E. coli*, *Escherichia coli*.

Population Coverage Analysis of the Multi-Epitope Vaccine

The population coverage of T-cell epitopes was estimated using the IEDB population coverage website. This prediction is crucial, as the success of vaccine development hinges on understanding the distribution of HLA alleles globally [31]. The analysis included 37 epitopes, with 12 designated for CTL and 25 for HTL. According to the results, 92.67% of the global population is covered by these 37 T-cell epitopes.

The highest coverage was observed in West Africa at 96.97%, while the lowest was in South Africa at 64.71%. Coverage rates in Southeast Asia and Indonesia were 89.69% and 81.12%, respectively. Other regions showed the following coverage percentages: East Asia (91.35%), South Asia (86.02%), Southwest Asia (87.58%), Europe (94.02%), East Africa (94.16%), Central Africa (91.71%), North Africa (90.24%), the West Indies (95.83%), Central America (73.25%), North America (96.05%), South America (86.23%), and Oceania (89.79%), as detailed in Figure S1.

Prediction of the Multi-Epitope Vaccine's Secondary Structure

The construction results of the multi-epitope vaccine candidate were uploaded to the PSIPRED server to obtain the 2D structure and to I-TASSER for the 3D structure analysis. The 2D structure of the vaccine predominantly consists of a random coil comprising 490 amino acids (45.97%), an alpha helix with 397 amino acids (37.24%), and an extended strand of 179 amino acids (16.79%) (Figure 2).

Tertiary Structure Modeling, Refinement, and Validation of Vaccine Construction

The 3D structural models of multi-epitope vaccine candidate constructs were predicted using the I-TASSER web tools [32,33]. We obtained 5 structural models with C-scores ranging from −5 to −0.96 (Table S4). Among these, model 1 exhibited the highest structural quality, as indicated by its superior C-score.

The 3D structural models of multi-epitope vaccine constructs, selected from the I-TASSER prediction results, were further refined using the GalaxyRefine web tools. The evaluation was based on RMSD and GDT-HA values [34], with higher values indicating superior quality [35]. Model 1 was selected based on the criteria. Significantly, the refined structure showed enhancements compared to the previous refinement, as presented in Figure S2. The improvement results were validated using ProSA Web and SAVEs, with assessment including ERRAT score and Ramachandran plot analysis, as shown in Figure 2 and Table 2 [36,37]. The ProSA analysis of model 1 indicated an improved Z-score, moving from 0.38 to −2.27 (Figure S2). Furthermore, analysis via a Ramachandran plot revealed that 76.5% of amino acid residues in model 1 were located in the most favored region. An ERRAT score exceeding 50 indicates superior model quality; for this vaccine construction, the score was 74.344, denoting convincing quality [36]. Ramachandran plot analysis of the model showed a score of 76.5% (Figure 3).

Prediction of Vaccine Solubility

The vaccine constructs were predicted to be soluble. As shown in Figure S3, the Protein-sol server generated a score >0.45 for a vaccine, compared to 0.45 for *E. coli* solubility. This result was further supported by predictions from the SOLpro webserver, which indicated solubility upon overexpression with a probability of 0. 988486 (>0.5).

Disulfide Characterization of the Vaccine

Engineering and analysis of disulfide bonds have been incorporated into vaccine structures to improve its stability by substituting highly potential residues with cysteine residues [15,17]. According to the results, 102 pairs of amino acids could potentially form disulfide bonds (Table S5). These pairs were further screened based on the chi^3 value (ranging from −87° to +97°) with a tolerance of 30 and a maximum Cα−Cβ−Sγ angle of 114.6°, as well as an energy value of less than 2.2. This screening process identified 6 pairs that were suitable for potential substitution with cysteine-cysteine residues. As shown in Figure 4, the pairs included Val29–

Figure 2. (A, B) Analysis of the secondary structure of *Mycobacterium tuberculosis* vaccine construct using PSIPRED webserver. (A) Sequence plot, (B) PSIPRED cartoon.

https://doi.org/10.24171/j.phrp.2024.0026

Table 2. Refinement and validation scores of the vaccine construct

Model	RMSD	GDT-HA	Z-score	ERRAT score	Ramachandran plot (%)
Model 1	0.504	0.9203	−2.27	74.344	76.5
Model 2	0.496	0.9219	−2.28	68.535	76.4
Model 3	0.490	0.9219	−2.29	73.216	76.7
Model 4	0.492	0.9235	−2.2	69.735	76.3
Model 5	0.503	0.9212	−2.11	67.169	77.3

RMSD, root-mean-square deviation; GDT-HA, global distance test high accuracy.

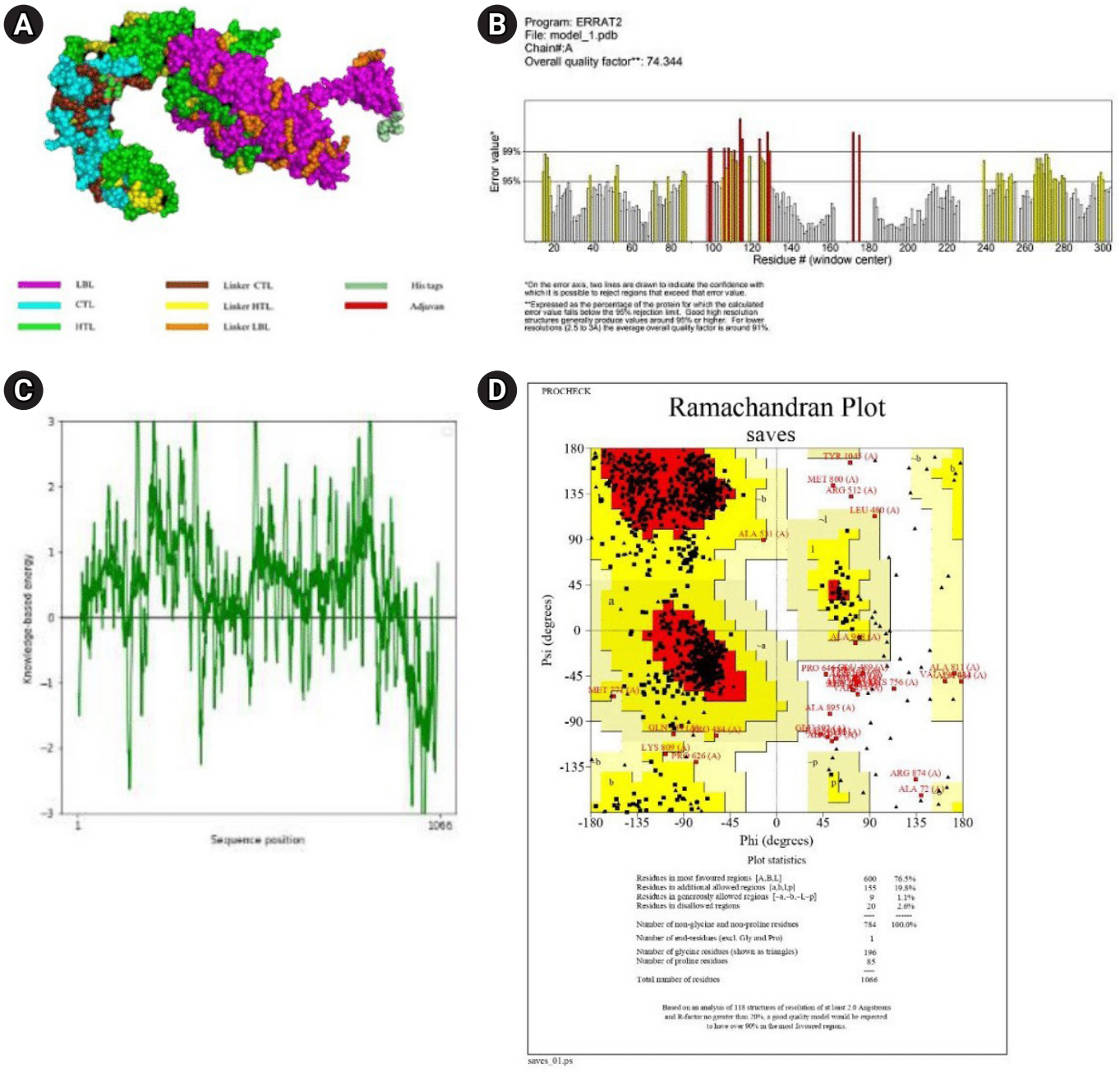

Figure 3. Refined 3-dimensional vaccine construction (A), Z-score (B), ERRAT values (C) and Ramachandran plots (D).

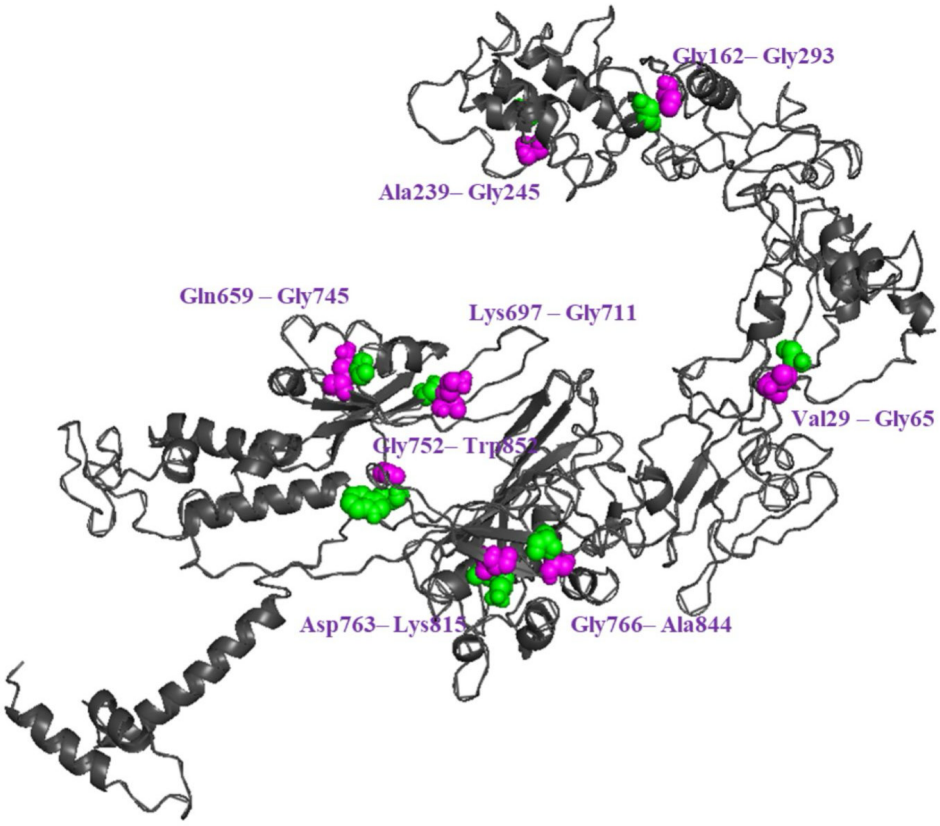

Figure 4. Disulfide engineering of the vaccine construct. Six pairs of potential residue that were mutated to cysteine residues to form disulfide bridges. Sequence of vaccine and annotation panels for predicting disulfide bonds.

Gly65, Gly162–Gly293, Ala239–Gly245, Gln659–Gly745, Lys697–Gly711, Gly752–Trp852, Asp763–Lys815, and Gly766–Ala844.

Analysis of Discontinuous B Cell Epitopes

Analysis of discontinuous B cell epitopes in the protein's 3D structure was crucial for understanding the interaction between the vaccine antigen and antibodies in organisms. These epitopes were also identified as antigenic sequences that could directly interact with receptors, thereby activating the immune system [13]. The analysis revealed 7 discontinuous B cell epitopes within the vaccine structure (Figure 5; Table 3). The scores of these epitopes ranged from 0.537 to 0.988, with each epitope consisting of between 3 and 388 residues.

Analysis of Active Sites in the Vaccine Construct

Identifying the active site of a protein is a crucial step before molecular docking because it helps predict the binding pocket of the ligand and protein [38]. Using the online tool CASTp, several potential pockets were identified in the vaccine construct. The most significant active site of the vaccine is shown in Figure 6, which has a pocket surface area of 7819.505 $Å^2$ and a volume of 15305.179 $Å^3$. These dimensions indicate its suitability for binding with TLR during molecular docking.

TLR and Multi-Epitope Tuberculosis Vaccine Construct Docking Studies

Analyzing the interactions between the vaccine construct and TLR is crucial for understanding how the vaccine interacts with endogenous immune receptors and for predicting its efficacy within the body [39]. Molecular docking was employed to analyze the interaction between 2 molecules and to identify the optimal orientation of a ligand within a complex [40]. In this study, molecular docking was used to evaluate how vaccine constructs interact with TLR2, TLR4, and TLR9. The 3D structures of TLR2 (2Z7X) [17], TLR4 (4G8A) [41], and TLR9 (5ZLN) [42] were obtained from the Protein Data Bank.

HADDOCK successfully generated 30 candidate models for each protein docking, including the TLR2 vaccine, TLR4 vaccine complex, and TLR9 vaccine complex, each with different binding energies. Among these models, the top-ranked complex for each protein exhibited the lowest

https://doi.org/10.24171/j.phrp.2024.0026

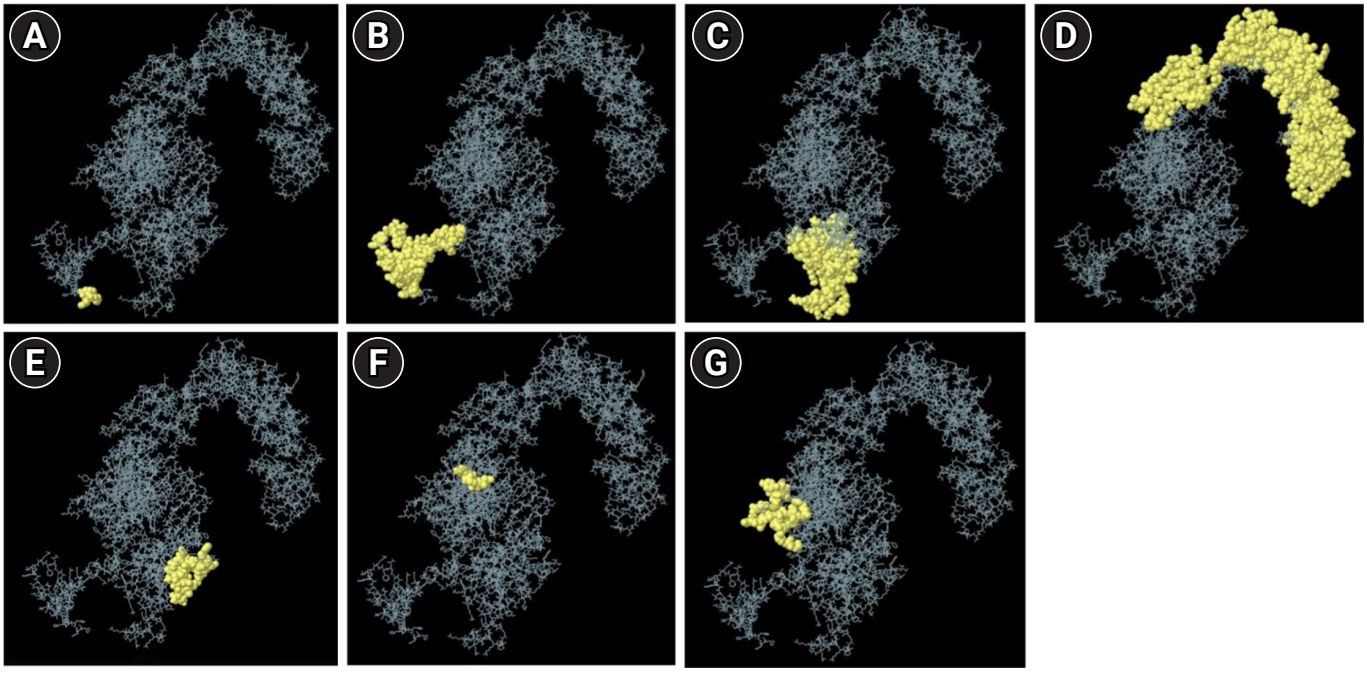

Figure 5. (A–G) The 3-dimensiional visualization of discontinuous B-cell epitopes. The yellow colour indicates the distribution of discontinuous B-cell epitopes in all sequences of the vaccine construct.

energies: –1,128.3 for TLR2, –1,332.5 for TLR4, and –1,352.0 for TLR9. These were further refined using HADDOCK 2.4, resulting in 100 water-refined versions. The docking demonstrated strong binding between TLR and the vaccine, with scores of –272.3 ± 1.0 for TLR2, –315.6 ± 8.7 for TLR4, and –360.4 ± 6.0 for TLR9 (Table 4). Advanced analysis using the PRODIGY web server to assess Gibbs energy (ΔG) and dissociation constant between the docked proteins revealed that the TLR9 vaccine complex was energetically the most favorable, featuring lower ΔG values of –25.2 kcal/mol and a dissociation constant of 3.6^{e-19}. The interaction between TLR and the vaccine involved hydrogen bonds, salt bridges, and non-bonded contacts (Figure 7). Additionally, docking of TLR with the vaccine using HDock generated multiple models. Consistent with previous findings, docked TLR9 exhibited the lowest energy scores, as presented in Table 4 [43,44].

Dynamic Molecular of Multi-Epitope Vaccine and MM-GBSA Calculation

Molecular dynamics of vaccine constructs are analyzed using NMA, which calculates internal coordinates by assessing collective functional motions and generating feasible transitions between 2 homologous structures on biological macromolecules. The results of the molecular dynamics for the TLR vaccine complex are detailed in Figure 8A–C. All 3 protein complexes exhibited multiple regions of high flexibility, as indicated by the peaks in the root mean square fluctuation, suggesting good flexibility. Meanwhile, other parameters, such as deformability, displayed varying patterns. In the variance plot, purple and green represent individual and cumulative variances, respectively. In the covariance matrix, the colors red, white, and blue denote correlated, uncorrelated, and anticorrelated movements, respectively. In the elastic network, darker gray areas indicate stiffer regions. Additionally, the eigenvalue of the vaccine construct varied, with the TLR2 vaccine complex showing lower values [45].

The complex was analyzed for binding free energy (ΔG_{bind}) to evaluate the favorability and affinity of protein-protein interactions in precise biological system modeling [13]. The TLR4 vaccine complex exhibited a lower binding free energy of – 159.52 kcal/mol. The corresponding residues for the ligand and receptors were PHE573 (–5.26 kcal/mol) and ARG105 (–9.77 kcal/mol), respectively (Table 5).

Codon Optimization and *In Silico* Cloning of the Vaccine

Codon optimization of the multi-epitope vaccine was performed using the Java Codon Adaptation Tool (JCat) server to maximize vaccine expression. In this study, an *E. coli* K-12 prokaryotic expression system with a time-

Table 3. The number of discontinuous B cell epitopes predicted, with the number of the residues and the scores in the constructed vaccine

No.	Residues	No. of residues	Score
1	A:H1064, A:H1065, A:H1066	3	0.988
2	A:R999, A:G1000, A:A1001, A:G1003, A:T1004, A:A1005, A:A1006, A:K1007, A:K1008, A:V1009, A:R1010, A:F1011, A:Q1012, A:E1013, A:A1014, A:A1015, A:N1016, A:K1017, A:Q1018, A:K1019, A:Q1020, A:K1021, A:L1022, A:D1023, A:E1024, A:K1025, A:K1026, A:E1027, A:M1028, A:K1029, A:T1030, A:D1031, A:A1032, A:A1033, A:T1034, A:L1035, A:A1036, A:Q1037, A:E1038, A:A1039, A:G1040, A:N1041, A:F1042, A:K1043, A:K1044, A:Y1045, A:R1047, A:A1048, A:D1049, A:E1050, A:E1051, A:Q1052, A:Q1053, A:Q1054, A:A1055, A:L1056, A:S1057, A:S1058, A:Q1059, A:M1060, A:H1061, A:H1062, A:H1063	63	0.87
3	A:N886, A:G887, A:T888, A:P889, A:N890, A:E891, A:L892, A:G893, A:G894, A:A895, A:N896, A:I897, A:P898, A:K899, A:K900, A:G901, A:D903, A:I904, A:Y913, A:Q914, A:S915, A:G916, A:K917, A:K918, A:P919, A:A920, A:F921, A:E922, A:W923, A:Y924, A:Y925, A:Q926, A:S927, A:G928, A:L929, A:S930, A:I931, A:V932, A:M933, A:P934, A:K935, A:K936, A:P937, A:T938, A:G939, A:S940, A:A941, A:A942, A:I943, A:G944, A:L945, A:S946, A:M947, A:A948, A:G949, A:S950, A:S951, A:A952, A:K953, A:K954, A:A955, A:N956, A:R957, A:A958, A:V959, A:K960, A:P961, A:T962, A:G963, A:S964, A:A965, A:A966, A:I967, A:G968, A:L969, A:S970, A:K971, A:K972, A:K973, A:W974, A:D975, A:A976, A:T977, A:A978, A:T979, A:E980	86	0.787
4	A:T13, A:C14, A:G15, A:G16, A:G17, A:G18, A:G19, A:G20, A:E21, A:A23, A:A24, A:G26, A:L27, A:P28, A:V29, A:E30, A:A35, A:A36, A:Y37, A:G38, A:P39, A:S40, A:L41, A:I42, A:G43, A:L44, A:A45, A:M46, A:A47, A:A48, A:Y49, A:R50, A:P51, A:G52, A:L53, A:P54, A:V55, A:E56, A:Y57, A:L58, A:A59, A:A60, A:Y61, A:N62, A:A63, A:A64, A:G65, A:G66, A:H67, A:N68, A:Y73, A:A74, A:A75, A:G76, A:G77, A:H78, A:N79, A:A80, A:V81, A:F82, A:A83, A:A84, A:Y85, A:G86, A:S87, A:A88, A:A89, A:I90, A:G91, A:L92, A:S93, A:M94, A:A95, A:A96, A:Y97, A:A107, A:A108, A:Y109, A:K112, A:T113, A:D114, A:A115, A:A116, A:T117, A:L118, A:A119, A:A120, A:Y121, A:T122, A:A123, A:A124, A:Q125, A:A126, A:A127, A:V128, A:V129, A:R130, A:A131, A:A132, A:Y133, A:G134, A:L135, A:P136, A:V137, A:E138, A:Y139, A:L140, A:Q141, A:V142, A:A143, A:A144, A:Y145, A:G146, A:L147, A:A148, A:G149, A:G150, A:A151, A:A152, A:T153, A:A154, A:A155, A:A156, A:Y157, A:A158, A:A159, A:T160, A:A161, A:G162, A:A163, A:F164, A:S165, A:R166, A:A167, A:A168, A:Y169, A:A170, A:M171, A:A172, A:S173, A:T174, A:E175, A:G176, A:N177, A:V178, A:A179, A:A180, A:Y181, A:T182, A:A183, A:A184, A:Q185, A:A186, A:A187, A:V188, A:V189, A:R190, A:A191, A:A192, A:Y193, A:E194, A:M195, A:K196, A:T197, A:D198, A:A199, A:A200, A:T201, A:L202, A:G203, A:P204, A:G205, A:P206, A:V211, A:G212, A:A213, A:V214, A:G215, A:G216, A:T217, A:A218, A:T219, A:A220, A:G221, A:A222, A:G223, A:P224, A:G225, A:P226, A:G227, A:A228, A:V229, A:V230, A:G231, A:L232, A:S233, A:M234, A:A235, A:A236, A:S237, A:S238, A:A239, A:L240, A:T241, A:L242, A:G243, A:P244, A:G245, A:P246, A:G247, A:G248, A:L249, A:V250, A:G251, A:A252, A:V253, A:G254, A:G255, A:T256, A:A257, A:T258, A:A259, A:G260, A:A261, A:F262, A:G263, A:P264, A:G265, A:P266, A:G267, A:L268, A:V269, A:G270, A:A271, A:V272, A:G273, A:G274, A:T275, A:A280, A:F281, A:S282, A:G283, A:P284, A:G285, A:P286, A:G287, A:G288, A:S289, A:A290, A:V291, A:V292, A:G293, A:L294, A:S295, A:M296, A:A297, A:A298, A:P304, A:G307, A:S308, A:A309, A:V310, A:V311, A:G312, A:L313, A:S314, A:M315, A:A316, A:A317, A:S318, A:S319, A:L321, A:T322, A:G323, A:P324, A:G325, A:P326, A:G327, A:L328, A:P329, A:V330, A:E331, A:Y332, A:L333, A:Q334, A:V335, A:P336, A:S337, A:S339, A:M340, A:G341, A:P344, A:G345, A:G347, A:V348, A:G349, A:A350, A:V351, A:G352, A:G353, A:T354, A:A355, A:T356, A:A357, A:G358, A:A359, A:F360, A:S361, A:R362, A:G363, A:P364, A:G365, A:P366, A:G367, A:V368, A:M378, A:G379, A:R380, A:D381, A:I382, A:G383, A:P384, A:G385, A:P386, A:G387, A:G388, A:L389, A:P390, A:V391, A:E392, A:Y393, A:L394, A:Q395, A:V396, A:P397, A:S398, A:P399, A:A416, A:G417, A:A418, A:F419, A:S420, A:R421, A:P422, A:G423, A:P424, A:G425, A:P426, A:G427, A:T428, A:G429, A:S430, A:A431, A:V432, A:V433, A:G434, A:L435, A:S436, A:M437, A:A438, A:A439, A:S440, A:S441, A:A442, A:G443, A:P444, A:G445, A:P446, A:G447, A:P448, A:T449, A:G450, A:S451, A:A452, A:V453, A:V454, A:L456, A:M458, A:A459, A:A460, A:S461, A:S462, A:G463, A:P464, A:I469, A:G470, A:T471, A:A473	388	0.681
5	A:L661, A:D662, A:G663, A:P664, A:G665, A:P666, A:G667, A:L668, A:G670, A:Q671, A:W672, A:G674, A:A675, A:A676, A:G677, A:T678, A:A679, A:A680, A:Q681, A:A682, A:K683, A:K684, A:A685, A:G686, A:G687, A:Y688, A:K689, A:G727, A:G728, A:G729, A:H730	31	0.568
6	A:R493, A:Q500, A:D501	3	0.566
7	A:R512, A:S513, A:S514, A:N515, A:L516, A:K517, A:Q519, A:A521, A:Y522, A:G523, A:P524, A:G525, A:L536, A:P537, A:G538, A:L539, A:V540, A:G541, A:L542, A:A591, A:I592, A:G593, A:L594, A:S595, A:F622, A:G623	26	0.537

dependent rho transcription terminator and prokaryotic ribosome binding sites was adopted for analysis. The CAI and GC values of the optimized nucleotide sequence in the multi-epitope vaccine with adjuvant were 99.63% and 55.95%, respectively. To validate the vaccine, a codon-optimized DNA sequence was inserted into the pET-28a(+) vector and cloned using the SnapGene application, with EcoRI and BamHI enzymes selected for the N- and C-terminal sites, respectively (Figure 9) [46].

https://doi.org/10.24171/j.phrp.2024.0026

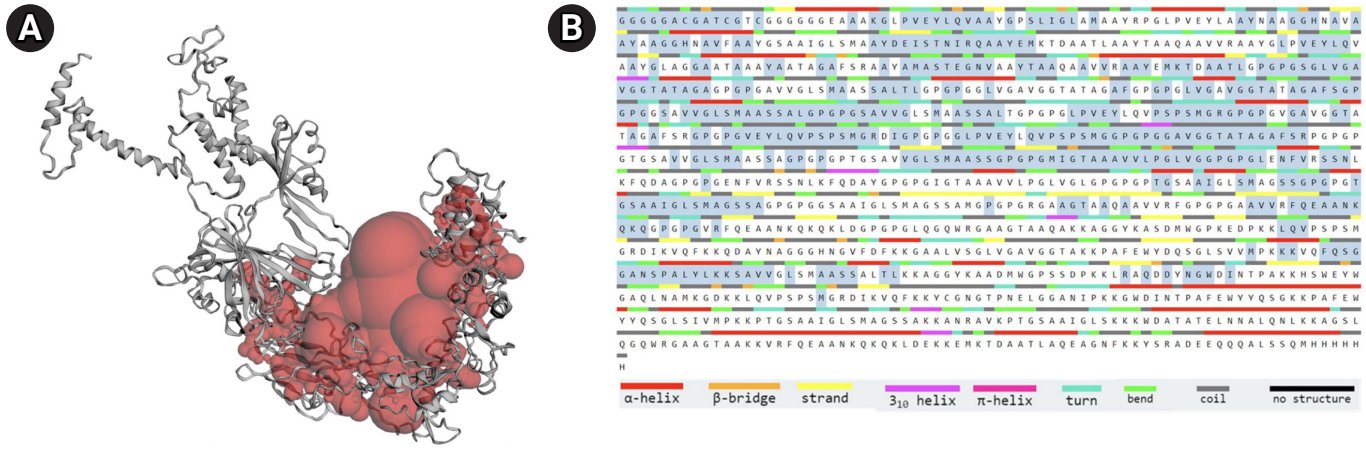

Figure 6. Active site prediction of the vaccine. (A) Best binding pocket/site (red colour sphere) of vaccine. (B) Sequence of vaccine and annotation panels in the vaccine construct.

Table 4. Result of docking of the vaccine with TLR2, TLR4, and TLR9

	TLR2 vaccine complex	TLR4 vaccine complex	TLR9 vaccine complex
Cluspro 2.0 webserver			
Center weighted score	−1,059.0	−1,181.6	−1,272.4
Lowest energy weighted score	−1,128.3	−1,332.5	−1,352.0
HADDOCK 2.4 webserver			
HADDOCK score	−272.3±1.0	−315.6±8.7	−360.4±6.0
RMSD from the overall lowest-energy structure	0.7±0.4	0.7±0.4	0.7±0.4
Van der Waals energy	−148.1±4.9	−165.2±4.7	−199.6±2.9
Electrostatic energy	−375.9±7.0	−537.9±50.8	−600.8±11.7
Desolvation energy	−49.0±5.1	−42.8±3.0	−40.7±3.9
Restraints violation energy	0.0±0.0	0.0±0.0	0.1±0.1
Buried surface area	4,385.9±41.8	5,597.0±51.4	5,804.3±64.5
ΔG (kcal/mol)	−16.5	−20.1	−25.2
K_d (M) at 25 °C	7.9^{e-13}	-18^{e-15}	3.6^{e-19}
HDock			
Docking score	−310.63	−332.58	−353.95
Confidence score	0.9613	0.9747	0.9834
Ligand RMSD (Å)	178.51	274.2	221.15

Values are presented as mean±standard deviation unless otherwise stated.
TLR, toll-like receptor; RMSD, root-mean-square deviation.

Immune Simulation of the Vaccine in Human Body Administration

Immune simulation analysis was conducted through the administration of 3 vaccine doses. These injections were administered on days 1, 28, and 56, maintaining a 4-week interval between each dose. Additionally, the vaccine was shown to be safe and to elicit immune responses involving B cells, T cells, and memory cells. Simulation of vaccine injection in humans showed an increase in the number of macrophages, B cells, and DCs (Figure 10). These cells play a crucial role in presenting antigens to T cells. The number of cytotoxic T cells and T helper cells also increased after 3 injections. Furthermore, there was a significant increase in the number of antibody-secreting plasma B cells following the third injection. This accounts for the elevated levels of serum IgM and IgG. Additionally, the injected vaccine construct influenced the proliferation of NK cells, which are part of the innate immune system and play a vital role in the elimination of intracellular pathogens [47].

Discussion

The emergence of antibiotic resistance in *M. tuberculosis* presents a significant threat to public health. Efforts to address this issue have included the development of new antibiotics or antimicrobials, but regulatory challenges and

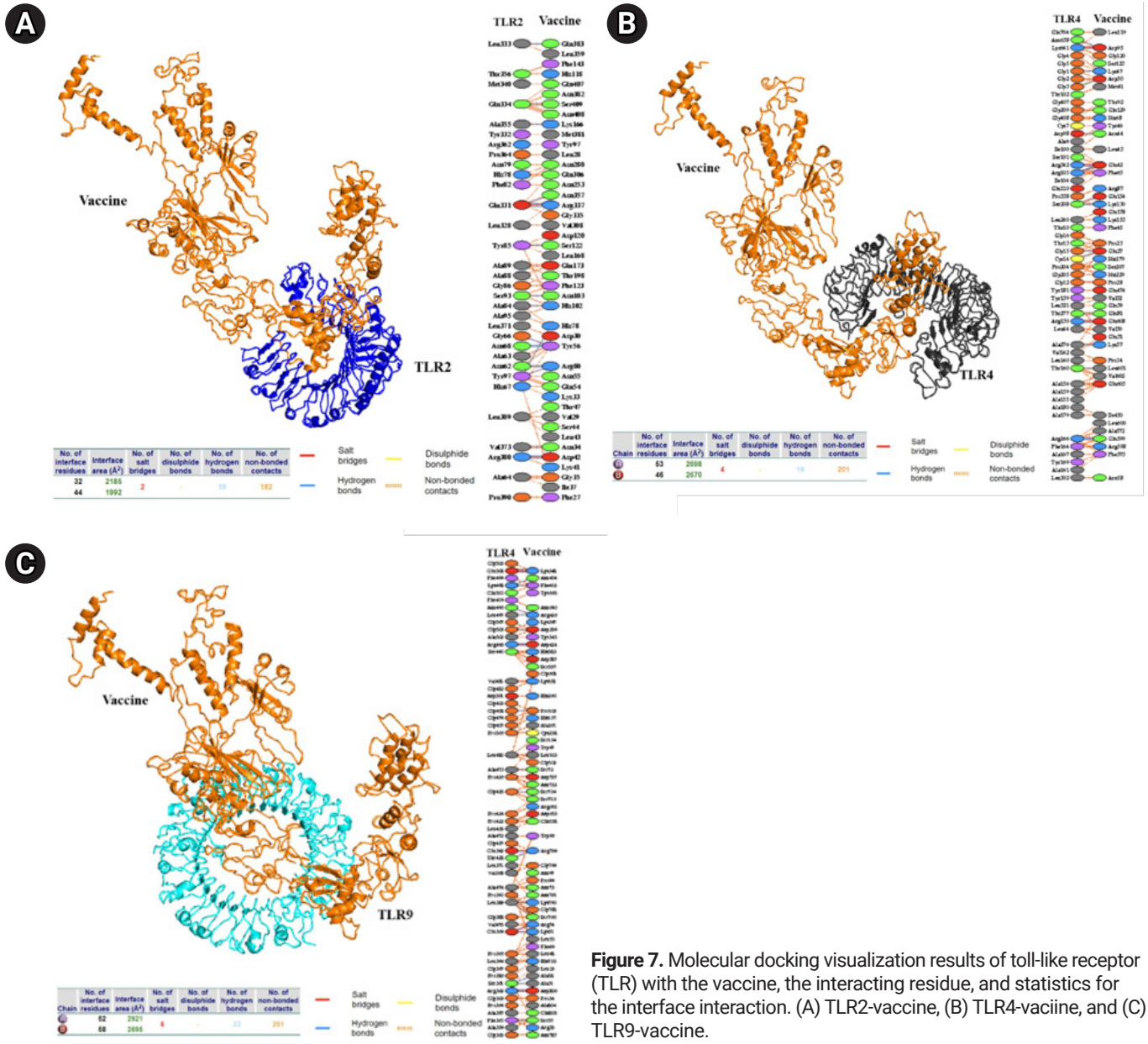

Figure 7. Molecular docking visualization results of toll-like receptor (TLR) with the vaccine, the interacting residue, and statistics for the interface interaction. (A) TLR2-vaccine, (B) TLR4-vaciine, and (C) TLR9-vaccine.

the high costs associated with drug development have cast doubt on their potential effectiveness. Vaccine development is a promising alternative. Although not all vaccines have proven effective against this issue, recent advancements, particularly in the use of multi-epitope-based vaccines and immunoinformatics approaches, have shown promising results [48–53].

Multi-epitope vaccines represent a novel strategy for addressing diseases caused by pathogens that rapidly develop resistance to current treatments. This type of vaccine employs a dual approach by incorporating elements that activate CTL, HTL, and LBL, thus simultaneously inducing robust humoral and cellular immune responses [22,54,55]. Enhancing vaccine constructs with suitable adjuvants boosts the immune response and extends the duration of protection [56]. In this context, a multi-epitope vaccine incorporating Ag85A, Ag85B, ESAT-6, and CFP-10 proteins was developed using an immunoinformatics approach. This vaccine construct offers multiple advantages over traditional vaccines. It includes a variety of MHC epitopes—specifically CTL, HTL, and LBL epitopes—that provide both therapeutic and prophylactic benefits. Furthermore, the addition of immunostimulants (adjuvants) significantly improves the vaccine's capacity to confer long-lasting

https://doi.org/10.24171/j.phrp.2024.0026

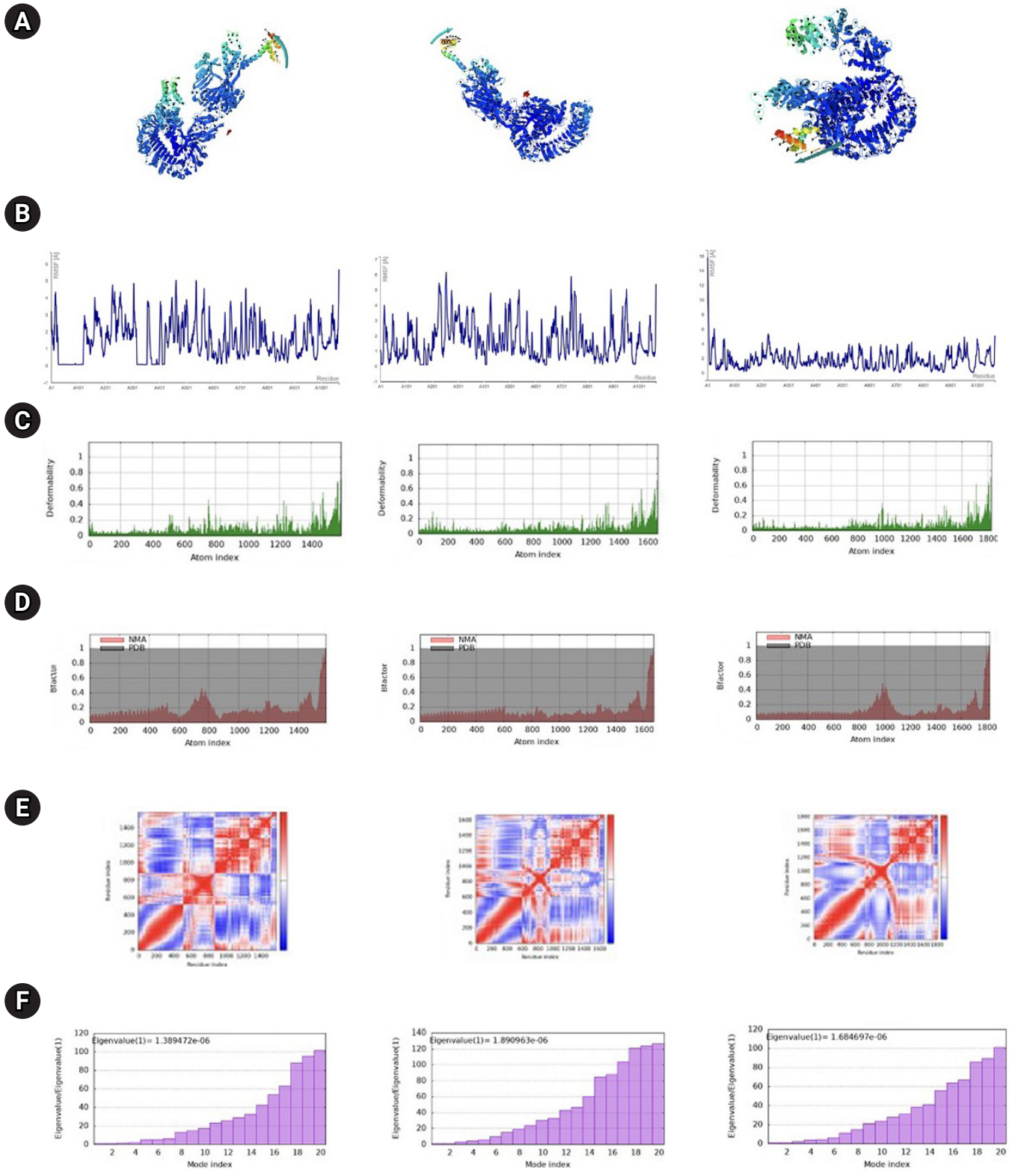

Figure 8. (Continued on next page.)

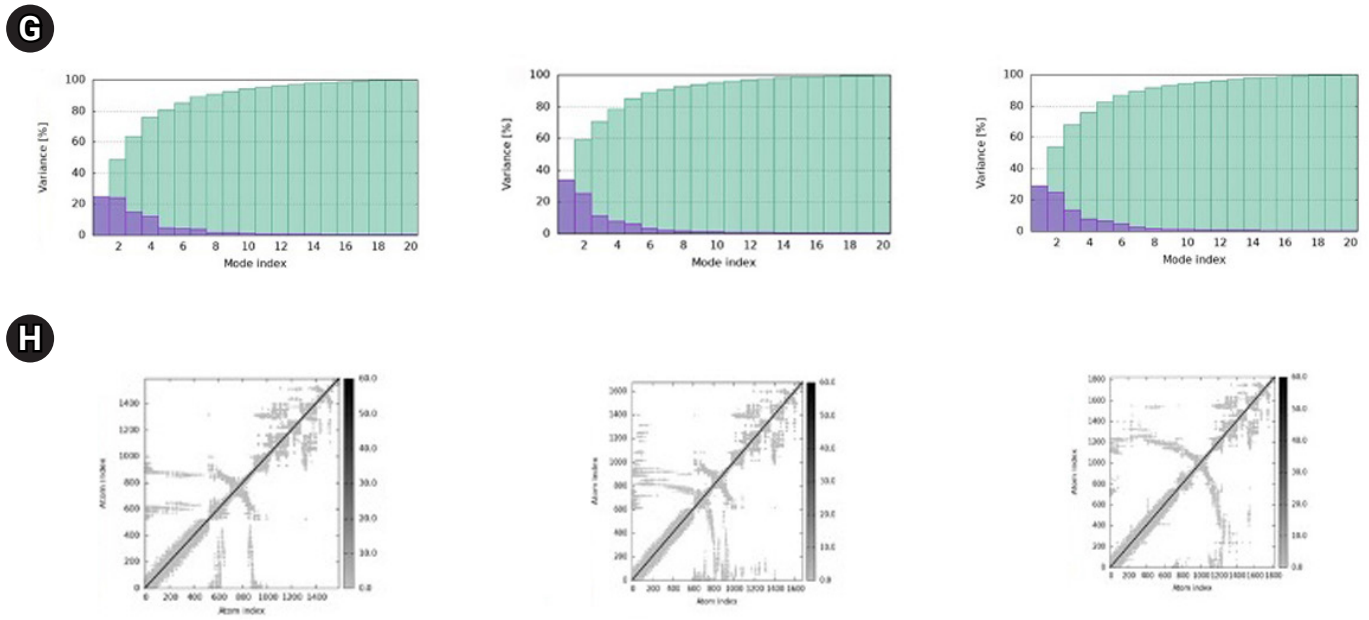

Figure 8. Molecular dynamic of toll-like receptro (TLR) with vaccine, including TLR2-vaccine, TLR4-vaccine, and TLR9-vaccine respectively (left to right). The direction of the motion (A), root mean square fluctuation (RMSF) (B), deformability (C), B(beta)-factor/ mobility (D), covariance map (E), eigen-value indicating the protein's normal mode and the stiffness of the motion (F), the normal mode variance (G), and elastic network (H).

immunity [57].

Previous studies have demonstrated that chimeric protein vaccines containing Ag85A, CFP-10, and ESAT-6 strengthen Th1 cytokine-expressing CD4+ responses. Additionally, other findings indicate that the CFP-10 protein is recognized by CD8+ cells with cytolytic activity *in vivo* against cells infected with *M. tuberculosis* [58]. The vaccine design developed in this study incorporates CTL, HTL, and LBL epitopes from Ag85A, Ag85B, ESAT-6, and CFP-10 proteins, with the goal of activating both adaptive and innate immune responses. The use of GPGPG (glycine-rich), KK, and AAY linkers is crucial for separating inter-epitopes. Glycine-rich linkers (GPGPG) enhance solubility, prevent the formation of junctional epitopes, and facilitate the immune processing of antigens [35]. AAY and GPGPG linkers also prevent cross-linking, which improves immunogenicity and epitope presentation. Additionally, KK linkers maintain the immunogenic activity of the epitope. Meanwhile, EAAAK linkers promote sustained immune responses [50,59]. Early in the vaccine construction, CpG adjuvants were added to stimulate adjuvant and innate immunity by activating B cells and DCs, thereby stimulating an effective immune response [60,61].

Epitopes selected for vaccine construction should exhibit immunodominant features, including immunogenicity and antigenicity, while minimizing allergenicity upon injection into the body [26,57]. These selected epitopes were then incorporated into the vaccine construct, which underwent further analysis for immunogenicity, allergenicity, antigenicity, and physicochemical properties. The 2D structure, characterized by a random coil and an α-helix, typifies an antigenic structural form. Modifications to the α-helix can enhance the immune system's binding to the protein [62]. The 3D structure of the vaccine construct was predicted using the I-TASSER web tools and refined with the GalaxyRefine web tools. GDT-HA and root-mean-square deviation (RMSD) serve as quality indicators following refinement. The refinement process involved adjusting and repositioning the side chains of the construct [63]. The Z-score from GalaxyRefine indicates the similarity of the vaccine construct's protein to experimental protein structures. A value within the typical range suggests the reliability of the vaccine construct's actual structure [64]. Additionally, the Ramachandran plot is used to verify quality post-refinement. Over 90% of the proteins were in the most favored and allowed regions, indicating the high quality of the designed vaccine construct [65,66]. This study identified 6 unstable regions in the structure of the vaccine construct, which were stabilized by forming disulfide bonds [15]. Observations indicated that the designed vaccine was thermostable, highly soluble, antigenic, and non-allergenic. These findings align with those of a previous study conducted by Abdulabbas et al. [67].

https://doi.org/10.24171/j.phrp.2024.0026

Table 5. MM/GBSA of results of protein-protein interaction with the top 10 lowest residues corresponding to binding and free energy binding

Protein	VDW	ELE	GB	SA	BFE total (kcal/mol)	Residue ligand	BFE (kcal/mol)	Residue/ receptor	BFE (kcal/mol)
TLR2 Vac	−216.86	111.44	3.63,	−27.37	−129.16	ARG-337	−8.26	TYR-97	−6.91
						TYR-56	−8.24	TYR-85	−6.47
						PHE-123	−4.57	GLU-331	−4.37
						GLN-306	−3.67	LEU-389	−4.33
						MET-381	−3.5	ARG-380	−3.9
						LEU-28	−3.41	PHE-82	−3.86
						ASP-42	−3.08	VAL-373	−3.00
						HIE-78	−2.87	ASN-62	−2.98
						ASN-357	−2.6	HIE-67	−2.91
						GLN-383	−2.35	GLN-334	−2.81
TLR4 Vac	−284.51	−3,368.52	3529.14	−35.63	−159.52	PHE-573	−5.26	ARG-105	−9.77
						ASP-95	−4.91	ARG-130	−7.82
						GLN-599	−4.48	ARG-342	−6.69
						PHE-63	−3.66	ILE-100	−6.00
						GLU-42	−3.49	ARG-166	−4.84
						VAL-30	−3.23	THR-13	−4.57
						GLU-608	−2.85	PRO-204	−4.42
						PRO-28	−2.74	THR-160	−3.85
						LEU-119	−2.74	PHE-164	−3.69
						PRO-34	−2.65	ALA-180	−3.48
TLR9 Vac	−309.81	2,582.22	−2,350.07	−37.16	−114.83	PRO-105	−6.13	LEU-389	−6.88
						PHE-402	−5.79	LEU-480	−6.54
						ARG-759	−5.03	PRO-366	−5.23
						ASP-424	−4.96	GLU-369	−4.78
						B-PHE-49	−4.83	GLU-508	−4.76
						B-ARG-74	−4.4	PRO-426	−4.54
						B-TRP-47	−4.03	SER-361	−4.43
						B-ASP-259	−3.99	ARG-362	−4.39
						B-SER-760	−3.94	VAL-475	−4.31
						B-ASP-806	−3.39	PRO-390	−3.91

VDW, van der Waals; GB, generalized Born; SA, surface area; BFE, binding free energy; TLR, toll-like receptor.

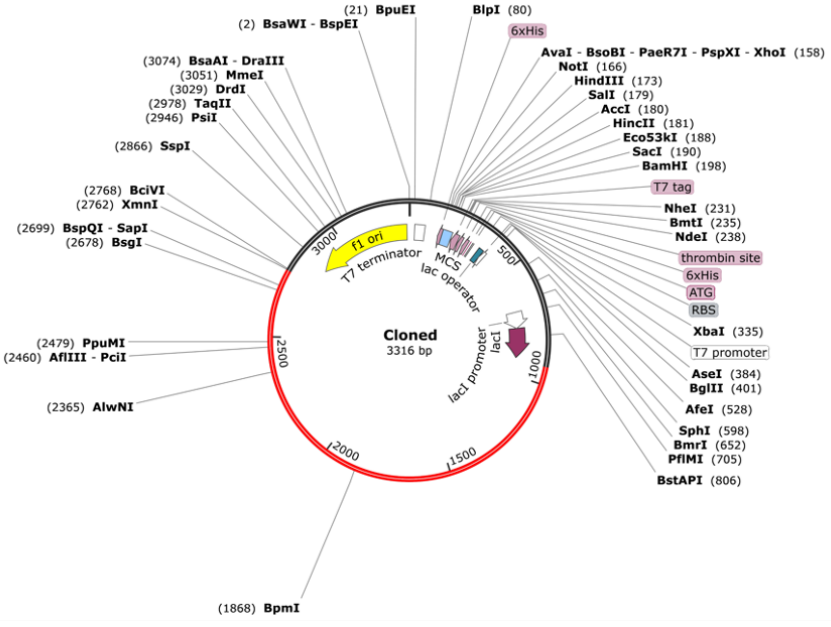

Figure 9. *In silico* cloning of the *Mycobacterium tuberculosis* candidate vaccine in a pET28a(+) vector. The red line indicate the inserted optimized DNA vaccine.

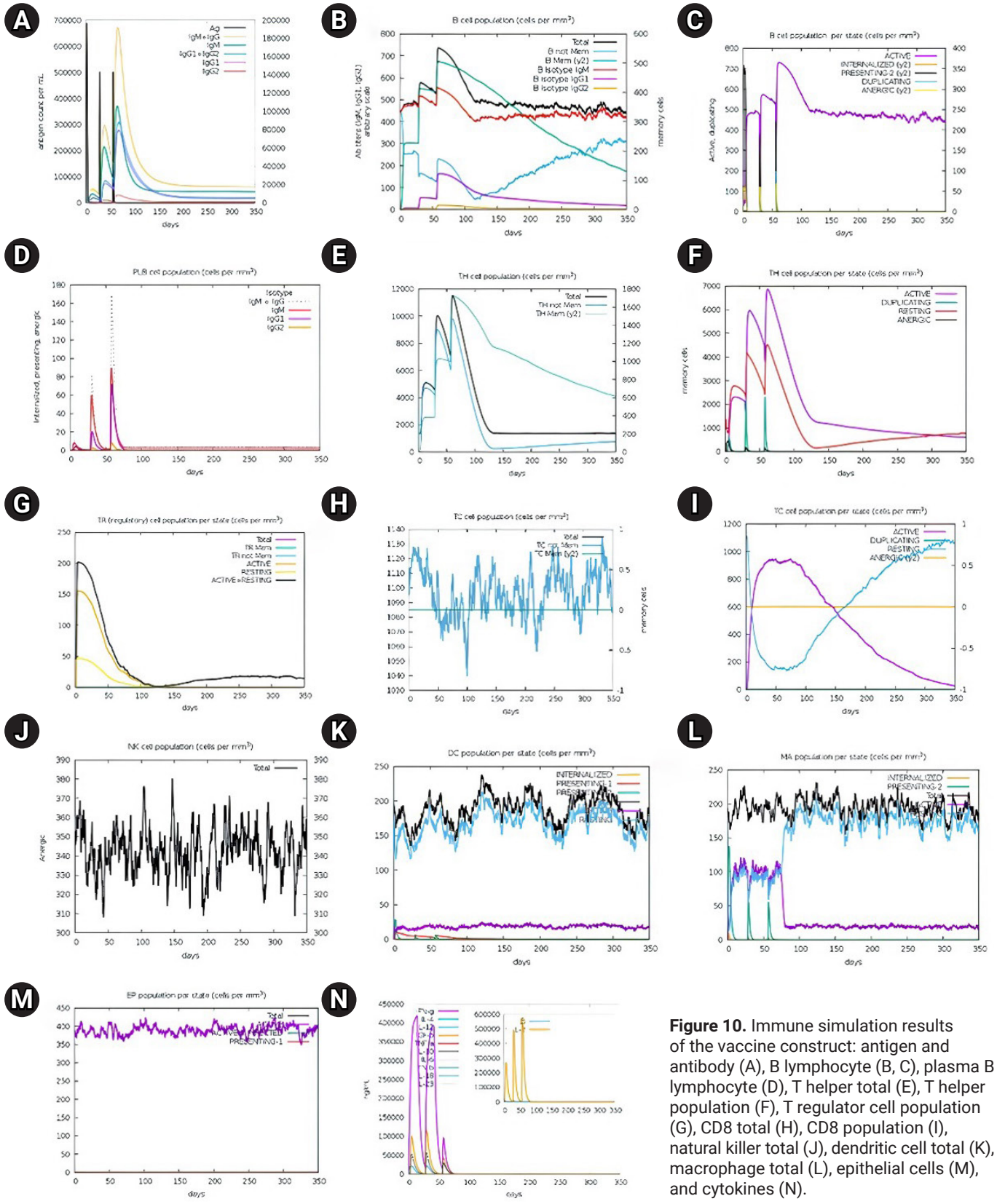

Figure 10. Immune simulation results of the vaccine construct: antigen and antibody (A), B lymphocyte (B, C), plasma B lymphocyte (D), T helper total (E), T helper population (F), T regulator cell population (G), CD8 total (H), CD8 population (I), natural killer total (J), dendritic cell total (K), macrophage total (L), epithelial cells (M), and cytokines (N).

https://doi.org/10.24171/j.phrp.2024.0026

The injected vaccine constructs should be capable of binding to receptors in the body. Therefore, molecular docking is necessary to ensure effective binding to target receptors, including TLR2, TLR4, and TLR9. TLR2 and TLR4 are surface receptors that are sensitive to recognizing circulating *M. tuberculosis* antigens. TLR2 plays a crucial role in inducing pathogen killing through macrophage activation [68]. Meanwhile, TLR4 facilitates the activation of Th1 cells via the activation of antigen-presenting cells (APCs) and DCs, leading to increased MHC-II expression and the induction of IL-12 and tumor necrosis factor (TNF)-α [69]. TLR9 contributes to the eradication of *M. tuberculosis* through a cross-presentation mechanism activated by CpG adjuvant, resulting in the production of IFN-α/β [69,70]. This mechanism is a vital component in the development of both therapeutic and prophylactic vaccines. A vaccine construct will have a therapeutic effect on an individual when it can: (1) enhance antigen uptake by APCs, (2) improve antigen processing and presentation by APCs, (3) enhance interaction between APCs and T cells, and (4) generate effective cytotoxic T cells and antibodies [71]. In this study, the vaccine construct was observed to bind intensely to 3 receptors: TLR2, TLR4, and TLR9 [6,48,49,67].

The immune simulation conducted in this study demonstrated an increase in the number of DCs and macrophages, which are crucial for the innate immune response involved in phagocytosing bacteria. Additionally, there was a significant increase in cytotoxic T cells, which are key effector cells against *M. tuberculosis* [58]. This suggests that the vaccine construct meets the necessary therapeutic criteria. The prophylactic efficacy was achieved by targeting humoral immunity, with B lymphocytes playing a pivotal role in generating this effect. Immune simulation analysis revealed an increase in the number of B lymphocytes that release IgM and IgG. This increase is closely linked to the activation of Th2 cells by APC cells, which are essential for the activation of B lymphocytes [71]. Furthermore, the T helper cell population increased during the immune simulation.

The results offer new hope for eradicating TB. The vaccine offers significant advantages over traditional options, such as lower cost and faster production, increased immunity potential and safety, reduced non-specific reactions or cross- reactivity, and easier manipulation [72]. Additionally, it is smaller and can trigger stronger immune responses due to a more potent immunogenic domain [73].

The designed vaccine warrants further validation through both *in vitro* and *in vivo* laboratory experiments. Jiang et al. [6] conducted recombination in the laboratory for the TB vaccine [74–76]. Additionally, various packaging approaches in the delivery system could be explored, including nanoparticle-based systems, which are known for their efficacy in delivering diverse genetic and protein materials [77–79]. An increasing body of evidence suggests that vaccine development adopting this approach has been widely successful both *in vitro* and *in vivo*, eliciting advanced immune responses and offering protection against some diseases. Jiang et al. [6] demonstrated that the design and recombination of a multi-epitope vaccine, named PP13138R, could increase the number of IFN-γ+ T cells and enhance cytokine production of TNF-α, IL-6, and IL-10 *in vitro* among isolated latent TB infection, active TB, and healthy controls. According to Kaushik et al. [76], the administration of multi-epitope vaccines in rabbits successfully induced antibody secretion against the dengue virus.

The results presented do not conclusively demonstrate the effectiveness of the vaccine in question. Proper antigen processing is essential for epitope immunogenicity, necessitating a comprehensive evaluation within the context of epitope delivery, typically via genetic constructs. This study provides sequences and spacing for CD8+ T cell and B cell epitopes; however, additional research is required to identify the optimal sequence and spacing for maximum immunogenicity. Most prediction tools fail to account for the precise location of antigen processing, which affects the prediction and presentation of epitopes. Furthermore, since the composition of antigen processing mechanisms can vary with proinflammatory signals and may differ across various cell types, current prediction algorithms might not be suitable for assessing the effectiveness of viral antigen processing in infected target cells.

Conclusion

In conclusion, a multi-epitope vaccine based on the Ag85A, Ag85B, ESAT-6, and CFP-10 proteins of *M. tuberculosis*, developed through an immunoinformatics approach, showed potential as both a prophylactic and therapeutic measure against TB. Global population coverage was estimated at 92.67%, with a coverage of 81.12% in Indonesia. The analysis indicated that the multi-epitope vaccine was immunogenic, antigenic, non-allergenic, and non-toxic. Additionally, it exhibited physicochemical characteristics that align with the parameters for potential vaccine manufacturing. The vaccine demonstrated a binding capability to TLR2, TLR4, and TLR9, which induced NK activity, activated macrophages, and DCs as APCs. It also stimulated T cells, B cells, and memory cells, and induced an increase in IgM and IgG antibodies following the administration of 3 doses. These attributes underscore the vaccine's ability to induce both innate and adaptive immune responses,

including the generation of memory cells for long-term protection.

Supplementary Material

Table S1. Results of the epitope prediction for the CTL proteins Ag85A, Ag85B, ESAT-6, and CFP-10; **Table S2.** Results of the epitope prediction for the HTL proteins Ag85A, Ag85B and CFP-10; **Table S3.** Results of the epitope prediction for the LBL proteins Ag85A, Ag85B, ESAT-6, and CFP-10; **Table S4.** Prediction of the 3D structure of the vaccine construct; **Table S5.** Disulfide bond of the vaccine; **Figure S1.** Population coverage of selected CTL and HTL epitopes worldwide; **Figure S2.** Visualization and Z-score of multi-the epitope vaccine constructed before and after refinement; **Figure S3.** Vaccine solubility prediction. Supplementary data are available at https://doi.org/10.24171/j.phrp.2024.0026.

Notes

Ethics Approval
Not applicable.

Conflicts of Interest
The authors have no conflicts of interest to declare.

Funding
This research was funded as a research in the Program Kreativitas Mahasiswa event by Direktorat Pembelajaran dan Kemahasiswaan (Belmawa) Ministry of Education, Culture, Research, and Technology.

Availability of Data
All data generated or analyzed during this study are included in this published article. For other data, these may be requested through the corresponding author. The datasets are not publicly available but are available from the corresponding author upon reasonable request.

Authors' Contributions
Conceptualization: AN, SEP; Data curation: AN, TS, MFN, DAC, RR; Formal analysis: AN, TS; Funding acquisition: AN, TS; Investigation: AN, TS, MFN; Methodology: AN, TS; Project administration: AN, TS; Resources: AN, DAC, MFN; Software: MFN, RR; Supervision: SEP, YY; Validation: SEP; Visualization: RR; Writing–original draft: AN, TS, DAC; Writing–review & editing: all authors. All authors read and approved the final manuscript.

References

1. World Health Organization (WHO) (CH). Global tuberculosis report 2023. WHO; 2023.
2. Perwitasari DA, Setiawan D, Nguyen T, et al. Investigating the relationship between knowledge and hepatotoxic effects with medication adherence of TB patients in Banyumas Regency, Indonesia. Int J Clin Pract 2022;2022:4044530.
3. Martinez L, Cords O, Liu Q, et al. Infant BCG vaccination and risk of pulmonary and extrapulmonary tuberculosis throughout the life course: a systematic review and individual participant data meta-analysis. Lancet Glob Health 2022;10:e1307–16.
4. World Health Organization Indonesia (WHO Indonesia) (ID). Indonesia TB Joint External Monitoring Mission (JEMM) report, 2022. WHO Indonesia; 2022.
5. United Nations Development Programme (UNDP) (US). UNDP Support to the Implementation of Sustainable Development Goal 3. UNDP; 2017.
6. Jiang F, Han Y, Liu Y, et al. A comprehensive approach to developing a multi-epitope vaccine against Mycobacterium tuberculosis: from in silico design to in vitro immunization evaluation. Front Immunol 2023;14:1280299.
7. Peng C, Tang F, Wang J, et al. Immunoinformatic-based multi-epitope vaccine design for co-infection of Mycobacterium tuberculosis and SARS-CoV-2. J Pers Med 2023;13:116.
8. Pitaloka DA, Izzati A, Amirah SR, et al. Multi epitope-based vaccine design for protection against Mycobacterium tuberculosis and SARS-CoV-2 coinfection. Adv Appl Bioinform Chem 2022;15:43–57.
9. Cobelens F, Suri RK, Helinski M, et al. Accelerating research and development of new vaccines against tuberculosis: a global roadmap. Lancet Infect Dis 2022;22:e108–20.
10. Atmaja RW, Nugraha J. Perbedaan antara jumlah sel T subset gamma-delta di darah tepi pada penderita tuberkulosis dan orang dengan latent tuberculosis infection. J Biosains Pascasarjana 2016;18:162–71. Indonesian.
11. Romano M, Squeglia F, Kramarska E, et al. A structural view at vaccine development against M. tuberculosis. Cells 2023;12:317.
12. Tkachuk AP, Bykonia EN, Popova LI, et al. Safety and immunogenicity of the GamTBvac, the recombinant subunit tuberculosis vaccine candidate: a phase II, multi-center, double-blind, randomized, placebo-controlled study. Vaccines (Basel) 2020;8:652.
13. Dey J, Mahapatra SR, Singh PK, et al. Designing of multi-epitope peptide vaccine against Acinetobacter baumannii through combined immunoinformatics and protein interaction-based approaches. Immunol Res 2023;71:639–62.
14. Tahir Ul Qamar M, Rehman A, Tusleem K, et al. Designing of a next generation multiepitope based vaccine (MEV) against SARS-COV-2: immunoinformatics and in silico approaches. PLoS One 2020;15:e0244176.
15. Elshafei SO, Mahmoud NA, Almofti YA. Immunoinformatics, molecular docking and dynamics simulation approaches unveil a multi epitope-based potent peptide vaccine candidate against avian leukosis virus. Sci Rep 2024;14:2870.
16. Shi J, Zhu Y, Yin Z, et al. In silico designed novel multi-epitope mRNA vaccines against Brucella by targeting extracellular protein BtuB and LptD. Sci Rep 2024;14:7278.
17. Zhu F, Tan C, Li C, et al. Design of a multi-epitope vaccine against six Nocardia species based on reverse vaccinology combined with immunoinformatics. Front Immunol 2023;14:1100188.
18. Shahab M, Aiman S, Alshammari A, et al. Immunoinformatics-

based potential multi-peptide vaccine designing against Jamestown Canyon Virus (JCV) capable of eliciting cellular and humoral immune responses. Int J Biol Macromol 2023;253(Pt 2):126678.

19. Hayat C, Shahab M, Khan SA, et al. Design of a novel multiple epitope-based vaccine: an immunoinformatics approach to combat monkeypox. J Biomol Struct Dyn 2023;41:9344–55.
20. Shahab M, Hayat C, Sikandar R, et al. In silico designing of a multi-epitope vaccine against Burkholderia pseudomallei: reverse vaccinology and immunoinformatics. J Genet Eng Biotechnol 2022;20:100.
21. Elshafei AM, Mahmoud NA, Almofti YA. Development of multi-epitopes vaccine against human papilloma virus16 using the L1 and L2 proteins as immunogens. Biosci Biotechnol Res Asia 2022;19:797–813.
22. Ysrafil Y, Imran AK, Wicita PS, et al. Mosaic vaccine design targeting mutational spike protein of SARS-COV-2: an immunoinformatics approaches. BioImpacts 2023 Jul 19 [Epub]. https://doi.org/10.34172/bi.2023.26443
23. Rencilin CF, Rosy JC, Mohan M, et al. Identification of SARS-CoV-2 CTL epitopes for development of a multivalent subunit vaccine for COVID-19. Infect Genet Evol 2021;89:104712.
24. Seedat F, James I, Loubser S, et al. Human leukocyte antigen associations with protection against tuberculosis infection and disease in human immunodeficiency virus-1 infected individuals, despite household tuberculosis exposure and immune suppression. Tuberculosis (Edinb) 2021;126:102023.
25. Jensen KK, Andreatta M, Marcatili P, et al. Improved methods for predicting peptide binding affinity to MHC class II molecules. Immunology 2018;154:394–406.
26. Panahi HA, Bolhassani A, Javadi G, et al. A comprehensive in silico analysis for identification of therapeutic epitopes in HPV16, 18, 31 and 45 oncoproteins. PLoS One 2018;13:e0205933.
27. Gupta S, Ansari HR, Gautam A, et al. Identification of B-cell epitopes in an antigen for inducing specific class of antibodies. Biol Direct 2013;8:27.
28. Ubi GM, Ikpeme EV, Essien IS. Essentials of the COVID-19 coronavirus. In: Kose U, Gupta D, de Albuquerque VH, et al., editors. Data science for COVID-19. Elsevier; 2022. p. 1–25.
29. Kalita P, Lyngdoh DL, Padhi AK, et al. Development of multi-epitope driven subunit vaccine against Fasciola gigantica using immunoinformatics approach. Int J Biol Macromol 2019;138:224–33.
30. Scheiblhofer S, Laimer J, Machado Y, et al. Influence of protein fold stability on immunogenicity and its implications for vaccine design. Expert Rev Vaccines 2017;16:479–89.
31. Bettencourt P, Muller J, Nicastri A, et al. Identification of antigens presented by MHC for vaccines against tuberculosis. NPJ Vaccines 2020;5:2.
32. Zheng W, Zhang C, Bell EW, et al. I-TASSER gateway: a protein structure and function prediction server powered by XSEDE. Future Gener Comput Syst 2019;99:73–85.
33. Zhou X, Zheng W, Li Y, et al. I-TASSER-MTD: a deep-learning-based platform for multi-domain protein structure and function prediction. Nat Protoc 2022;17:2326–53.
34. Shin WH, Lee GR, Heo L, et al. Prediction of protein structure and interaction by GALAXY protein modeling programs. Bio Des 2014;2:1–11.
35. Sanami S, Rafieian-Kopaei M, Dehkordi KA, et al. In silico design of a multi-epitope vaccine against HPV16/18. BMC Bioinformatics 2022;23:311.
36. Andongma BT, Huang Y, Chen F, et al. In silico design of a promiscuous chimeric multi-epitope vaccine against Mycobacterium tuberculosis. Comput Struct Biotechnol J 2023;21:991–1004.
37. Messaoudi A, Belguith H, Ben Hamida J. Homology modeling and virtual screening approaches to identify potent inhibitors of VEB-1 β-lactamase. Theor Biol Med Model 2013;10:22.
38. Meng XY, Zhang HX, Mezei M, et al. Molecular docking: a powerful approach for structure-based drug discovery. Curr Comput Aided Drug Des 2011;7:146–57.
39. Ghandadi M. An immunoinformatic strategy to develop new Mycobacterium tuberculosis multi-epitope vaccine. Int J Pept Res Ther 2022;28:99.
40. Sanami S, Azadegan-Dehkordi F, Rafieian-Kopaei M, et al. Design of a multi-epitope vaccine against cervical cancer using immunoinformatics approaches. Sci Rep 2021;11:12397.
41. Ohto U, Yamakawa N, Akashi-Takamura S, et al. Structural analyses of human Toll-like receptor 4 polymorphisms D299G and T399I. J Biol Chem 2012;287:40611–7.
42. Ishida H, Ohto U, Shibata T, et al. Structural basis for species-specific activation of mouse Toll-like receptor 9. FEBS Lett 2018;592:2636–46.
43. Desta IT, Porter KA, Xia B, et al. Performance and its limits in rigid body protein-protein docking. Structure 2020;28:1071–81.
44. Mitra D, Pandey J, Jain A, et al. In silico design of multi-epitope-based peptide vaccine against SARS-CoV-2 using its spike protein. J Biomol Struct Dyn 2022;40:5189–202.
45. Jyotisha, Singh S, Qureshi IA. Multi-epitope vaccine against SARS-CoV-2 applying immunoinformatics and molecular dynamics simulation approaches. J Biomol Struct Dyn 2022;40:2917–33.
46. Dey J, Mahapatra SR, Patnaik S, et al. Molecular characterization and designing of a novel multiepitope vaccine construct against Pseudomonas aeruginosa. Int J Pept Res Ther 2022;28:49.
47. Murphy K, Weaver C. Janeway's immunobiology. 9th ed. Garland Science; 2016.
48. Farhani I, Yamchi A, Madanchi H, et al. Designing a multi-epitope vaccine against the SARS-CoV-2 variant based on an immunoinformatics approach. Curr Comput Aided Drug Des 2024;20:274–90.
49. Malik M, Khan S, Ullah A, et al. Proteome-wide screening of potential vaccine targets against Brucella melitensis. Vaccines (Basel) 2023;11:263.
50. Ullah A, Rehman B, Khan S, et al. An In silico multi-epitopes vaccine ensemble and characterization against nosocomial Proteus penneri. Mol Biotechnol. 2023 Nov 7 [Epub]. https://doi.org/10.1007/s12033-023-00949-y.
51. Safavi A, Kefayat A, Abiri A, et al. In silico analysis of transmembrane

protein 31 (TMEM31) antigen to design novel multiepitope peptide and DNA cancer vaccines against melanoma. Mol Immunol 2019; 112:93–102.

52. Safavi A, Kefayat A, Mahdevar E, et al. Exploring the out of sight antigens of SARS-CoV-2 to design a candidate multi-epitope vaccine by utilizing immunoinformatics approaches. Vaccine 2020;38:7612–28.
53. Safavi A, Kefayat A, Sotoodehnejadnematalahi F, et al. In silico analysis of synaptonemal complex protein 1 (SYCP1) and acrosin binding protein (ACRBP) antigens to design novel multiepitope peptide cancer vaccine against breast cancer. Int J Pept Res Ther 2019;25:1343–59.
54. Zhang L. Multi-epitope vaccines: a promising strategy against tumors and viral infections. Cell Mol Immunol 2018;15:182–4.
55. Ysrafil Y, Sapiun Z, Astuti I, et al. Designing multi-epitope based peptide vaccine candidates against SARS-CoV-2 using immunoinformatics approach. Bioimpacts 2022;12:359–70.
56. Ojha R, Pareek A, Pandey RK, et al. Strategic development of a next-generation multi-epitope vaccine to prevent Nipah virus zoonotic infection. ACS Omega 2019;4:13069–79.
57. Rafi MO, Al-Khafaji K, Sarker MT, et al. Design of a multi-epitope vaccine against SARS-CoV-2: immunoinformatic and computational methods. RSC Adv 2022;12:4288–310.
58. Woodworth JS, Wu Y, Behar SM. Mycobacterium tuberculosis-specific CD8+ T cells require perforin to kill target cells and provide protection in vivo. J Immunol 2008;181:8595–603.
59. Tahir Ul Qamar M, Shokat Z, Muneer I, et al. Multiepitope-based subunit vaccine design and evaluation against respiratory syncytial virus using reverse vaccinology approach. Vaccines (Basel) 2020; 8:288.
60. Bode C, Zhao G, Steinhagen F, et al. CpG DNA as a vaccine adjuvant. Expert Rev Vaccines 2011;10:499–511.
61. Coffman RL, Sher A, Seder RA. Vaccine adjuvants: putting innate immunity to work. Immunity 2010;33:492–503.
62. Corradin G, Villard V, Kajava AV. Protein structure based strategies for antigen discovery and vaccine development against malaria and other pathogens. Endocr Metab Immune Disord Drug Targets 2007;7:259–65.
63. Asghari A, Majidiani H, Nemati T, et al. Toxoplasma gondii tyrosine-rich oocyst wall protein: a closer look through an in silico prism. Biomed Res Int 2021;2021:1315618.
64. Heydari Zarnagh H, Hassanpour K, Rasaee MJ. Constructing chimeric antigen for precise screening of HTLV-I infection. Iran J Allergy Asthma Immunol 2015;14:427–36.
65. Al-Khayyat MZ, Al-Dabbagh AG. In silico prediction and docking of tertiary structure of LuxI, an inducer synthase of Vibrio fischeri. Rep Biochem Mol Biol 2016;4:66–75.
66. MohammedSalih KA, Khalil AA, Musa AM, et al. Role of toll like receptor 2 and 4 (TLR2 and TLR4) in susceptibility and resistance to Mycobacterium tuberculosis infection among Sudanese patients. Arch Microbiol Immunol 2020;4:11–25.
67. Abdulabbas HT, Mohammad Ali AN, Farjadfar A, et al. Design of a novel multi-epitope vaccine candidate against Chlamydia trachomatis using structural and nonstructural proteins: an immunoinformatics study. J Biomol Struct Dyn 2024;42:4356–69.
68. Thada S, Horvath GL, Muller MM, et al. Interaction of TLR4 and TLR8 in the innate immune response against Mycobacterium tuberculosis. Int J Mol Sci 2021;22:1560.
69. Chuang YC, Tseng JC, Huang LR, et al. Adjuvant effect of Toll-like receptor 9 activation on cancer immunotherapy using checkpoint blockade. Front Immunol 2020;11:1075.
70. Simmons DP, Canaday DH, Liu Y, et al. Mycobacterium tuberculosis and TLR2 agonists inhibit induction of type I IFN and class I MHC antigen cross processing by TLR9. J Immunol 2010;185:2405–15.
71. Cheng MA, Farmer E, Huang C, et al. Therapeutic DNA vaccines for human papillomavirus and associated diseases. Hum Gene Ther 2018;29:971–96.
72. Behmard E, Abdulabbas HT, Abdalkareem Jasim S, et al. Design of a novel multi-epitope vaccine candidate against hepatitis C virus using structural and nonstructural proteins: an immunoinformatics approach. PLoS One 2022;17:e0272582.
73. Alibakhshi A, Alagheband Bahrami A, Mohammadi E, et al. In-silico design of a new multi-epitope vaccine candidate against SARS-CoV-2. Acta Virol 2024;67:12481.
74. Tang XD, Guo SL, Wang GZ, et al. In vitro and ex vivo evaluation of a multi-epitope heparinase vaccine for various malignancies. Cancer Sci 2014;105:9–17.
75. Safavi A, Kefayat A, Mahdevar E, et al. Efficacy of co-immunization with the DNA and peptide vaccines containing SYCP1 and ACRBP epitopes in a murine triple-negative breast cancer model. Hum Vaccin Immunother 2021;17:22–34.
76. Kaushik V, G SK, Gupta LR, et al. Immunoinformatics aided design and in-vivo validation of a cross-reactive peptide based multi-epitope vaccine targeting multiple serotypes of dengue virus. Front Immunol 2022;13:865180.
77. Li Y, Zhu Y, Sha T, et al. A multi-epitope chitosan nanoparticles vaccine of Canine against Echinococcus granulosus. J Biomed Nanotechnol 2021;17:910–20.
78. Abdul Rahman NA, Mohamad Norpi AS, Nordin ML, et al. DENV-mimetic polymersome nanoparticles bearing multi-epitope lipopeptides antigen as the next-generation dengue vaccine. Pharmaceutics 2022; 14:156.
79. Ysrafil Y, Astuti I, Anwar SL, et al. MicroRNA-155-5p diminishes in vitro ovarian cancer cell viability by targeting HIF1α expression. Adv Pharm Bull 2020;10:630–7.

https://doi.org/10.24171/j.phrp.2024.0026